



Tide-driven microplastics transport in an elongated semi-closed bay: A case study in Xiangshan Bay, China



Mingchao Yin ^a, Haijin Cao ^{a,*}, Wenlu Zhao ^b, Teng Wang ^a, Wei Huang ^c, Minggang Cai ^d

^a College of Oceanography, Hohai University, Nanjing 210024, PR China

^b School of Environmental Science and Engineering, Zhejiang Gongshang University, Hangzhou 310018, PR China

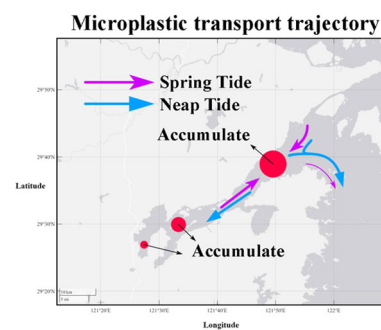
^c Key Laboratory of Marine Ecosystem and Biogeochemistry, Second Institute of Oceanography, Ministry of Natural Resources, Hangzhou 310012, PR China

^d College of Ocean and Earth Science, Xiamen University, Xiamen 361005, PR China

HIGHLIGHTS

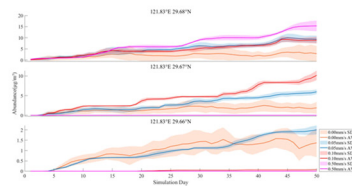
GRAPHICAL ABSTRACT

- On-site microplastics observations in the Xiangshan Bay show medium abundance.
- The release location is crucial to microplastic transport under tidal impacts.
- The inner bay accumulates microplastics during spring tide, as opposed to the outer.



Abundance: 890.6 ± 419.4 (particles/m³)

Settling velocity cannot be ignored



ARTICLE INFO

Editor: Dimitra A. Lambropoulou

Keywords:

Microplastics transport
Tidal flow
Numerical modelling

ABSTRACT

Coastal bays are important containers for plastic wastes before they enter the ocean. Based on field samples, this study presents the main characteristics of microplastics and uses a numerical model to study the distribution and movement of microplastics as they are driven by tidal flows in an extended semi-closed bay in Xiangshan Bay, China. The laboratory analyses of microplastic samples from 27 pollutant source samples collected in three batches provided fundamental data on microplastics. Our results show that the local microplastics are prevalent (mean abundance: 890.6 ± 419.4 particles/m³) in the water. A higher quantity of fibre- and fragment-type microplastics was identified and compared to other plastic types. The detected microplastics varied in colour and composition. The simulation suggests that the bay can trap microplastics inside it, with only 16.92 % discharged into the open ocean. A series of single-source numerical tests at nine typical observation sites were conducted to examine tide-driven microplastic transport. Our results suggest that the release location is crucial to microplastic distribution. Specifically, the microplastics tended to accumulate near the bay mouth and the Tie inlet; the microplastics released from the north shore generally evacuated the bay more easily; and the inner harbour tended to accumulate microplastics during spring tide, as opposed to the departure of microplastics at the outer bay, while the effect was reversed during neap tide. We further considered the deposit effect, which significantly reduces the discharging rate to 0.04 % with a settling velocity of 0.05 mm/s. These results may have great importance to decision-making, management, and control of microplastic pollution.

1. Introduction

Plastic pollution is now a critical environmental issue, and its discharge into the ocean has caused severe global damage to marine ecosystems. Global plastic production has reported to approach 360 million ton (Plastics Europe, 2020). Plastic pollution in the ocean is estimated to

* Corresponding author at: College of Oceanography, Hohai University, 1 Xikang Road, Nanjing 210024, PR China.

E-mail address: h.cao@hhu.edu.cn (H. Cao).

account for approximately 60 %–80 % of marine garbage, and up to approximately 90 %–95 % in some areas (Moore, 2008). With the increasing plastic production, global riverine plastic outflow is projected to peak in 2028 (Mai et al., 2020). Plastics in the ocean often draw attention because they are easy to spot, and the fate of plastic debris is significant. Plastics with sizes <5 mm are commonly called microplastics (MPs) and are formed by the fragmentation of larger-sized plastic pieces (Ekerkes-Medrano et al., 2015). MPs can follow ocean flows and be transported over long distances, causing them to have been detected in water columns, polar sea ice, and sediments (Kara et al., 2010; Eriksen et al., 2013a; Van Cauwenberghe et al., 2013; Law et al., 2014; Peeken et al., 2018; Cunningham et al., 2020; Kanhai et al., 2020). The ubiquity of MPs has severe ecological implications. MPs easily absorb waterborne harmful substances, such as heavy metals and persistent organic pollutants (Teuten et al., 2007; De Tender et al., 2015; Brennecke et al., 2016). After being ingested by organisms, MPs would enter the food chain and eventually appear in food, threatening human health (Jabeen et al., 2017; Prata et al., 2020; Walkinshaw et al., 2020). Nanoscale plastics can cross the placenta and blood-brain barrier and be absorbed by the gastrointestinal tract and lungs, damaging human health (Seltenrich, 2015).

On-site sampling is currently the primary method for studying MP pollution; however, some observations may be accidental because the sampling process directly affects the accuracy of the observed data (Liu et al., 2019). Additionally, the seawater MP distributions are affected by hydrodynamic conditions (such as tides, eddies). However, fixed-point, long-term, and real-time MPs observations, such as buoy observations, are impossible under current technical conditions. Recently, the development and maturity of ocean-based numerical models have provided a new method for studying oceanic physical processes, material transport, pollutant diffusion, and other issues (McWilliams, 2000). Previous studies have used numerical models to simulate the horizontal transport (Siegfried et al., 2017; Kaandorp et al., 2020) and vertical processes (Kooi et al., 2017) of MPs, such as Regional Ocean Modelling System (ROMS) (Cohen et al., 2019; Pereiro et al., 2019), HYbrid Coordinate Ocean Model (HYCOM) (Lebreton et al., 2012, 2018; Isobe et al., 2019), and Estuarine Coastal Ocean Model (ECOM) (Zhang et al., 2020a).

As they are produced by human activity, MPs primarily enter the ocean through rivers. Therefore, coastal areas are vital in controlling the spread of MPs. Many similar studies have focused on estuaries and bays (Chen et al., 2018; Dai et al., 2018; Chen et al., 2020; Genc et al., 2020; Wu et al., 2020a; Zhao et al., 2020). However, previous studies have mainly focused on analysing the existence and ecotoxicity of MPs in bays. Often, when discussing spatial distribution or transport, less attention is given to the background flow field, leading to haphazard results.

Many factors affect MP transportation in estuarine environments, including tides, runoff, wind (Claessens et al., 2011; Kukulka et al., 2012; Vianello et al., 2013; Wu et al., 2020b; Zhang et al., 2020b), degradation, biofilm deposition and other (Kooi et al., 2017; Tu et al., 2020), among which are the most important physical processes (Wang et al., 2016). Degradation, biofilm deposition, and other factors also affect the movement of MPs. Biofilm formation and degradation affect MP densities, but act on a significantly longer time scale (Tu et al., 2020; Kaandorp et al., 2020) than hydrodynamic processes.

A typical semi-closed bay in Zhejiang Province, China, the Xiangshan Bay (XSB), was selected as the study area. Considering the limitations of our observations, that is, the abundances obtained from the sampling points in this study could not represent the MP spatial distribution in the entire XSB, we further used numerical simulations to analyse the spatiotemporal MP distributions in the surface water of the XSB. The bay was identified as an area that easily contains MPs through quantitative MPs migration analyses. The numerical simulation is an appropriate choice to add to this study to remedy the data deficiency caused by the discontinuity of sampling time.

Therefore, this study has several main focuses, including reporting the MP characteristics in the XSB, simulating the spatial distribution and migration of MPs under tidal forcing, and assessing the settling effects of the MPs.

2. Methods

2.1. Study area

The XSB (Fig. 1), located on the north coast of Zhejiang Province and southeast of Ningbo, is between 29°24'–29°46' N and 121°25'–122°00' E, with a total length and average width of approximately 60 and 10 km, respectively. It is a narrow, long, and semi-closed bay extending inland from the northeast to the southwest. The narrowing in the middle of the bay is a significant feature, and divide the bay into two harbour areas. There are three inner ports in the XSB with frequent aquaculture and shipping activities.

Surrounded by low mountains and hills, there are limited runoffs ($\sim 12.89 \times 10^8 \text{ m}^3$) and wind or wave effects in the XSB (Gao et al., 1990; Chen, 1992). Tides (mainly semi-diurnal constituent) in the XSB propagate from the East China Sea to the elongated bay and result in water and material exchange between the bay and open ocean (Xu et al., 2016; Li et al., 2017; Yang et al., 2018). Tidal asymmetry plays an essential role in pollutant transport in the XSB. Tides have regular frequency and phases that can be easily predicted. Therefore, in the numerical simulation section, we will focus on the tidal influence on MP movement, which is beneficial for deepening our understanding of the basic law of MPs transport.

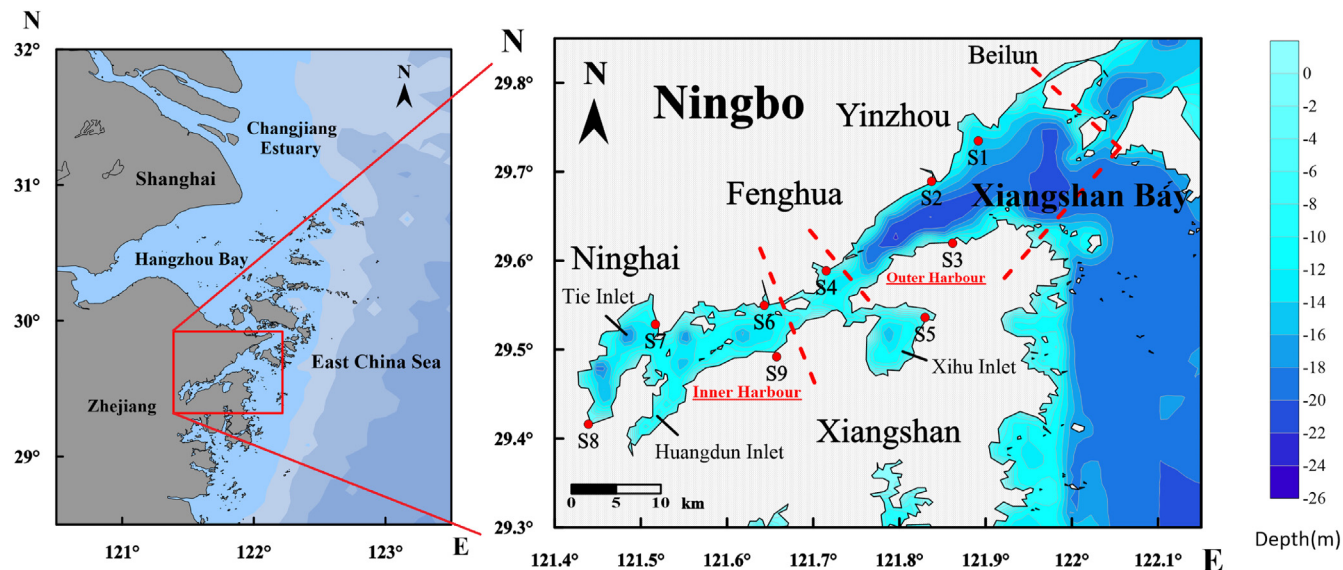


Fig. 1. The geographical location of XSB and the MPs sampling sites (S1–S9), with red dash lines dividing the XSB into the outer and inner harbour.

2.2. Sampling and analysis

Field sampling was conducted during October 2018, March 2019, and July 2019. The sampling site was selected near the drainage sluice along the coast, and approximately 20 L of nearshore surface water was collected using a stainless-steel bucket (<0.5 m). Filtration was completed through a stainless-steel sieve ($d = 5 \text{ mm}$) and nylon sieve silk ($d = 45 \mu\text{m}$), and distilled water was used to wash the devices (Tang et al., 2018; Zhao et al., 2020). Finally, the sieve silk was stored in 500 mL glass bottles, and the sampling time and site were marked. All devices were rinsed with distilled water before sampling. Nine sites were sampled for MP analyses. Sites S1 and S5 were slightly adjusted during the following two samples, considering the environmental conditions.

In the laboratory, sieve silk was removed from the glass bottle and placed in a 2 L glass beaker. The sieve silk was soaked in distilled water and the beaker was placed in an ultrasonic cleaning device for 5 min to transfer all particles in the sieve silk to distilled water. The silk sieve was rinsed with distilled water in a beaker and then filtered onto nylon filters (Millipore, 20 μm) for drying. Each nylon filter was then placed in a membrane box. A portable microscope was used to photograph the suspected MPs on the filter membrane, and their colour, shape, size, and quantity were recorded. A micro-Fourier transform infrared spectrometer (μ -FTIR) (Nicolet 10, Thermo Fisher Scientific, USA) was used to identify the polymer type of the MPs (Tang et al., 2018; Zhang et al., 2019). Cooling by liquid nitrogen, MPs were identified by μ -FTIR in transmission mode. The spectral range and aperture size range from 650 to 4000 cm^{-1} (64 co-scans at a resolution of 8 cm^{-1}) and 50 \times 50 μm to 150 \times 150 μm (depending on the size of the suspected MPs we choose), respectively. When the matching degree between the obtained spectra and OMNIC polymer spectrum library is >70 %, the suspected MPs are identified as specific polymer types (Wu et al., 2020a).

2.3. Quality control

The same method was used to complete two blank control groups at the laboratory and sampling sites. Blank samples were filtered with 20 L of Milli-Q water instead of seawater. All the tools were flushed at least three times with Milli-Q water before use, and all reagents were prepared using Milli-Q water and were filtered through filters (20 μm). Before the experiment, all glass bottles containing the samples were sealed and kept in a freezer to avoid interference from the environment (Zhao et al., 2020).

Pollution control measures were also implemented during these analyses. To avoid secondary contamination, lab coats and nitrile gloves were worn until laboratory work was completed and the experimental platform was sanitised with alcohol. The laboratory supplies were immediately covered with aluminium foil when not in use. All sample results were modified with blank groups to reduce the interference of the laboratory and sampling environment on the samples (Wang et al., 2019a).

2.4. Numerical simulation

In this study, based on the third batch (July 2019) of sampling results, a numerical model, MIKE 21 Flow Model FM (MIKE Powered by DHI), was used to simulate the MP migration in the XSB during 13 July and 1 September, with a 900-s time step. In total, 58,828 triangular grids were included in the study area. The minimum spatial resolution is ~50 m (coast), and the maximum spatial resolution is ~1 km (bay mouth). A simulation time of 50 days can include periodic changes in the tides and reduce the deviations between the simulation and reality caused by biofouling (Tu et al., 2020), among other factors.

The offshore tidal variations from the Tide Model Driver (TMD) (Erofeeva et al., 2020) were used as the open boundary condition. Observations at the tide station inside the bay (Xize Station, 121.833°E, 29.617°N) were used to validate the simulated tides (National Marine Data Center, 2019). The tidal range was slightly larger than the observations and the phase remained the same. Water depth was based on a local sea chart.

Because the sampling was completed near the discharge sluice, it could be approximated as the MP point source input of the model. As the flux of the discharge sluice changes irregularly, the results are expressed as percentages to analyse the situations of each discharge source. The discharge of each source in the model was estimated by the abundance, density, and volume of MPs, and the flux of the sluice. This study primarily focused on polyethylene (PE) (proportion in the third batch result: 9.77 %), one of the most common types of MPs in the environment (Andrady, 2011), with a density less than that of seawater and can stay in surface seawater for a significant amount of time. The wind drives the seawater to mix. MPs abundances in surface water (<0.5 m) are higher with a lower wind speed (Kukulka et al., 2012; Reisser et al., 2015). Due to the weak wind and wave conditions in the XSB, it is feasible to choose PE to simulate the MPs transport in surface water.

3. Results and discussion

3.1. Observation

3.1.1. Abundance

MPs were detected in all water samples collected from the XSB. The average abundance for these three batches ranged from 812.7 ± 409.0 to 988.9 ± 398.7 particles/m³, with an overall average is 890.6 ± 419.4 particles/m³ (Table 1). The highest mean abundance was in the first batch, followed by that in the third batch. In this study, the MP abundance in the XSB was a medium abundance. The different lower limits of size and sampling methods significantly affected the results. Compared with previous studies on a similar lower limit of size, our results were higher than those in Jiaozhou Bay (46 ± 28 particles/m³) (Zheng et al., 2019).

Although the MP abundances in the XSB obtained by trawl sampling was only 8.91 ± 4.70 particles/m³ (Chen et al., 2018), such a visible difference is possibly because the sampling method and the lower size limit differed. Additionally, for the numerical simulation, the sampling sites in this study were selected near the drainage gate, and the water samples may contain more MPs. The trawl sampling results in the XSB (Chen et al., 2018) were generally higher than those in the Bohai Sea (Zhang et al., 2017), Yellow Sea (Sun et al., 2018), South China Sea (Cai et al., 2018), and other areas. We speculate that this can be attributed to the openness of these areas. MP abundances are likely to be higher in seawater near the coast or in cities with high population densities (Zhao et al., 2014). The following discussion in the numerical simulation section further proves the rationality of this assumption: the MPs enrichment was led by the low openness of the XSB.

We also found that most sites exhibited clear seasonal changes (Fig. 2). S1 showed high MP abundance in all three batches. S2, S7, and S8 showed significant differences, with obvious seasonal differences among the different batches. Beilun and Yinzhou are the primary distribution areas of the plastic market, with dense populations and high terrestrial MPs inputs, which may affect S1 and S2. Large areas of mariculture exist in Ninghai and Xiangshan, and many buoyancy devices increase the offshore input of MPs (SI. 2).

3.1.2. Microplastic characteristics

Four shapes and seven colours of MPs were observed across the three batches of samples (Fig. 2). MP shapes in the XSB were dominated by fibres and fragments, contributing 25.42 % and 47.10 % of the total MPs in the first batch, 53.56 % and 27.06 % in the second batch, and 43.26 % and 29.38 % in the third batch, respectively. White was the primary colour composition, and the maximum proportion reached 76.48 % (S9-A).

Based on the FTIR spectroscopy results, 18 polymer types were detected (SI. 3). In the surface water of the XSB, polyethylene terephthalate (PET) and cellulose occupy the vast majority of polymer types, with average proportions of >17.33 % and 13.9 %, respectively. In each batch, the sums of the PET and cellulose contents were between 40 % and 70 %. These polymers are generally used in water bottles, plastic boxes, and other daily

Table 1

Comparison of microplastic abundance in the XSB with other studies.

Study area	Sampling method	Lower limit of size (μm)	Abundance (particles/m ³)	Reference
North Atlantic subtropical gyre	Trawl	300	5000–360,000 n/km ²	(Brach et al., 2018)
South Pacific subtropical gyre	Trawl	333	26,898 n/km ²	(Eriksen et al., 2013b)
Western Mediterranean Sea	Trawl	330	129,682 n/km ²	(Faure et al., 2015)
Arctic polar waters	Trawl	333	0.34 ± 0.31	(Lusher et al., 2015)
Black Sea	Trawl	200	1100 ± 900	(Aytan et al., 2016)
Bohai Sea	Trawl	300	0.33 ± 0.34	(Zhang et al., 2017)
Xiangshan Bay	Trawl	333	8.91 ± 4.70	(Chen et al., 2018)
Yellow Sea	Trawl	500	0.13 ± 0.20	(Sun et al., 2018)
East China Sea	Trawl	333	0.167 ± 0.138	(Zhao et al., 2014)
Yangtze River Estuary	Pump	32	4137.3 ± 2461.5	
South China Sea	Trawl	333	0.045 ± 0.093	(Cai et al., 2018)
	Pump	44	2569 ± 1770	
Yangtze River in Wuhan	Pump	50	1660.0 ± 639.1–8925 ± 1591	(Wang et al., 2017)
Longjiao Bay	Pump	20	1594.2 ± 1352.2	(Chen et al., 2020)
Bohai Sea	CTD	20	7667 ± 7271	(Dai et al., 2018)
	Stainless steel bucket	20	2200 ± 1387	
Maowei Sea	Stainless steel bucket	20	4500 ± 100	(Zhu et al., 2019)
Jiaozhou Bay	Stainless steel bucket	20	46 ± 28	(Zheng et al., 2019)
Qiantang River	Stainless steel bucket	47	1183 ± 269	(Zhao et al., 2020)
Xiangshan Bay	Stainless steel bucket	47	988.9 ± 398.7 (2018.10) 812.7 ± 409.0 (2019.3) 870.2 ± 430.4 (2019.7) 890.6 ± 419.4 (overall average)	This study

products. Additionally, some polyolefin components have a high proportion, such as PE with an average ratio of 9.77 % and polypropylene (PP)-polyethylene copolymer (E/P) with an average ratio of 14.42 %. These polymer materials have a low density and may be used in aquaculture products, such as cages, buoyancy materials, and fishing lines (Wang et al., 2016). The XSB is one of the largest aquaculture bays in China. PE, PET, PP, and polystyrene are common MP polymers in this coastal China environment (Wang et al., 2019b; Yu et al., 2022), which were also detected in this study. Contrarily, some types of MP polymers are relatively rare in the XSB surface water and much less abundant in the environment; therefore, there are phenomena detected in one batch and not detected in another batch. Note that the in-situ observation results (MP abundance, colour, shape, and composition) can be influenced by many factors including seasonal domestic laundry wastewater discharge, fishing moratorium, and natural factors (e.g., precipitation) (Browne et al., 2011).

3.2. Numerical results

3.2.1. Spatial distribution of microplastics

The simulation results show that MPs can spread to most regions of the XSB under continuous discharge from nine sources (Fig. 3a). The outer harbour showed a relatively higher MP concentration than other places. In the central channel, the lower MP concentration may be due to the fast flow velocity that transports the MPs away. The MP concentration in most areas of the inner harbour was slightly lower than that in the outer harbour. There appears to be a prominent accumulation in the Tie inlet and the areas of islands because of the slow velocity in these areas.

The MP input magnitude from each source point correlates with the observations (SI. 1). In the simulation, a high-abundance area appeared at the bay mouth because of the high input from S1, S2, and S3. The MP abundances of these three sources were at the top of the list in the third batch of results (July 2019). After an approximately 20-day simulation, the MPs started to leave the bay, and the distribution of MPs in the bay tended to stabilise. Until day 50, the main difference was mostly the increase in abundance values due to the continuous input of MPs. These results also indicate that MPs tended to accumulate in the bay.

Simulations with each single emission source were conducted to compare the tidal effects on MPs transport at different release locations (Fig. 3b). The results showed that the MPs from most sources would occupy the entire bay, except S1, S3, and S8. The MPs from S1 and S3 can be easily carried away from the bay (Fig. 3b). However, S8, which is in the innermost part of the bay, is not significantly affected by tides. The MPs released from

S1 (the easternmost emission source) mainly stayed at the bay mouth and left the XSB in the southeast direction. S2 and S3 are on the opposite side of the bay, near the bay mouth, exhibiting different influences on MPs transport (i.e., MPs from both S2 and S3 can move out of the bay, but only those from S2 can enter the inner harbour area). S4, S6, and S9 are in the middle of the bay, and MPs can spread rapidly throughout the bay over a short period (less than five days). The MPs released at the Xihu inlet (S5) could easily spread throughout the bay. The MPs distribution by S7 showed significant accumulation near the Tie inlet due to weak tidal action, and only a small number of MPs reached the outer harbour area after 20 days. In the case of S8, most MPs accumulated in the southern area of the Tie inlet, suggesting that the MPs from S8 were the least affected by tides. However, field observations did not detect an extremely high abundance value from surface water at this site; meaning that the MPs at S8 may be diffused for other reasons (e.g., settling, as discussed in the following section).

The latest observations support our numerical simulation results (XSB, sampling time: 2019.05) (Yu et al., 2022), showing similar MPs distribution in the areas (near the Tie Inlet and S2). The difference of MPs abundance between the observations and simulations are owing to the limited simulating time. The high abundance values in the sediments of Tie Inlet indicate that the MPs released by S7 and S8 may tend to settle down there. Similar sampling results have been found in previous studies (Chen et al., 2018). MPs transport model in a bay located in the Mediterranean Sea indicates that the phenomenon of MPs accumulation exists in some places with weak ocean currents (Genc et al., 2020). Therefore, sources near the Tie Inlet where tidal action is weak deserve attention.

The discussion of individual sources clarifies the differences caused by the geographical location of point sources: the bay mouth is conducive to the departure of MPs, the middle of the bay and north shore are conducive to the diffusion of MPs, and MPs released from the innermost bay will remain in the XSB for a longer period. Although the distribution of sources may have an impact on the formation of accumulation areas, the MPs are transported as particles by the flows, so the MPs from one single source point won't be largely different from the case with several source points. These phenomena are related to the characteristics of the flow field in the bay and will be discussed further.

3.2.2. Microplastics transport by tidal flow

The flow field is an essential factor in the distribution of MPs (Zhang et al., 2020a; Zhang et al., 2020b). Because tidal flow is a typical reverse flow, the flow velocity is highly asymmetric during flood and ebb tides

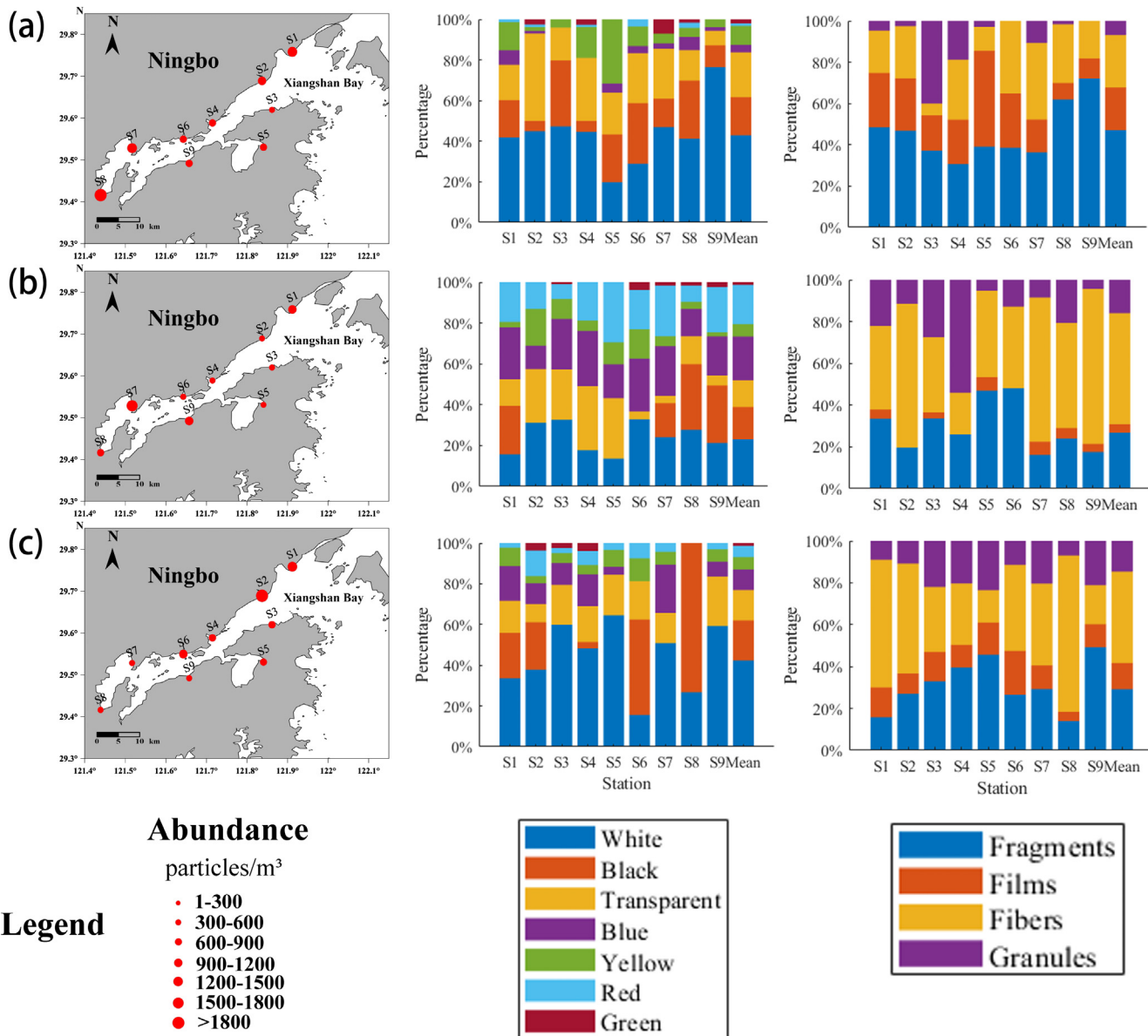


Fig. 2. Microplastic abundances (left), shapes (middle), and colours (right) in the XSB. (a) Sampling results of 2018.10; (b) sampling results of 2019.3; and (c) sampling results of 2019.7. The abscissa of the histogram indicates stations (S1–S9 and Mean) and the ordinate indicates percentages (0–100 %).

under the influence of topography, which also differs between sites (i.e., the current ellipse in Fig. 4c). The current ellipses at Points 1, 2, and 4 indicate a tendency of the seawater to approach the south bank, which drives the MPs toward the south bank as well. MPs from the north side are prone to long-distance migration, whereas those from the south bank tend to become stranded. The island and the constant inflow of seawater caused vortices to form around Point 4 during the ebb and flood tides. The vortical flow patterns during high and low tides serve as a barrier for MPs transport, preventing the MPs from leaving the bay along the north side (Fig. 4b). As such, the south side is the most important runaway route for MPs to the open ocean. After leaving the XSB, MPs will be transported to different seas by the Zhejiang and Fujian coastal current in different seasons (Zhang et al., 2020a). The distribution of MPs may also be correlated with the salinity fronts formed by tidal mixing of seawater (Cohen et al., 2019).

Different tidal stages would also affect MPs transport because of the different asymmetries in tidal velocity at different points (Wu et al., 2020b). At Point 2, the ebb tide shows a greater velocity than the flood tide, whereas the opposite is true for Point 3 (Fig. 4c). Thus, after a tidal period, the

MPs at Points 2 and 3 tended to be transported eastward and westward, respectively, by asymmetric tide flow. This may prevent the MPs exchange between the inner and outer harbours. However, the MPs between the two points can still be exchanged when the proper release timing is selected. Specifically, MPs released during the flood tide near Point 2, or during the ebb tide near Point 3, can pass through the narrow channel between the two points. These results are of great importance for the management and control of MP pollution in the bay.

The transformation between spring and neap tides is the third influencing factor. This study analysed the fate of MPs released from each source during the spring and neap tides (Fig. 5a). Except for S7 and S8, the results of each source were significantly different. MPs accumulated in the outer harbour area during spring tide and moved out of the XSB in large quantities during neap tide. The maximum self-purification rate of MPs during spring tide was only approximately 45 % (Fig. 5a, S2). However, during the neap tide, the self-purification rate of the same source was as high as approximately 143 % (Fig. 5a, S2), suggesting that the neap tide was beneficial for the outer harbour to purify its MP pollution. For the inner harbour, changes in the net increase in MPs suggest that spring tides can

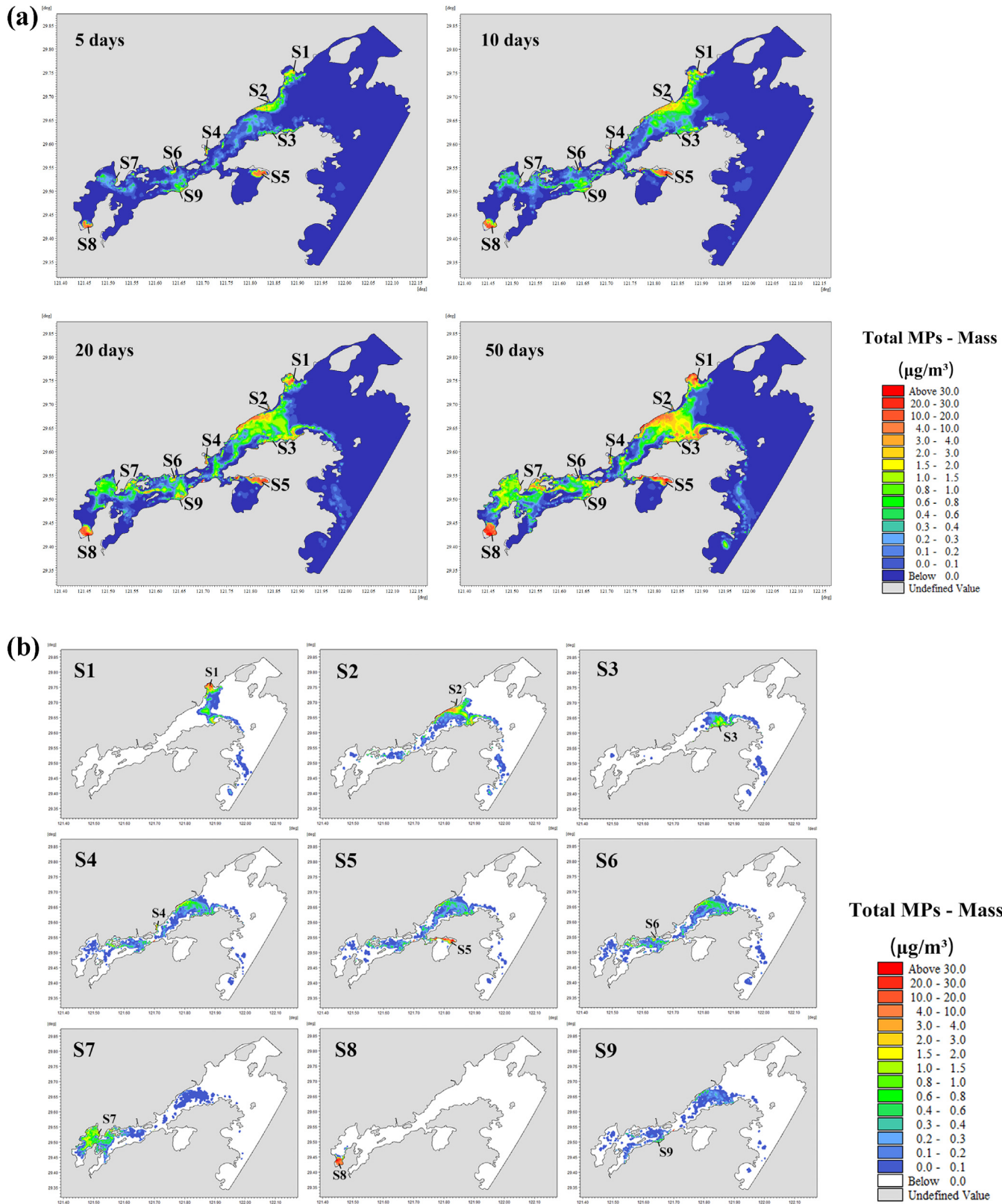


Fig. 3. Spatial distribution of MPs by 9 sources (a) and single-source (b).

help MPs leave the inner harbour; however, MPs accumulated in the outer harbour area after leaving the inner harbour area. They can hardly move out of the XSB until the self-purification capacity of the outer harbour is enhanced during the neap tide. Notably, the effects of the source location

mentioned above are shown more concretely here. The south shore (S3) is less efficient in moving the MPs out of the bay; S1 on the north shore, the self-purification rate of S1 is similar to, or even weaker than, that of S2 during the spring tide, although S1 is closer to the mouth of the bay.

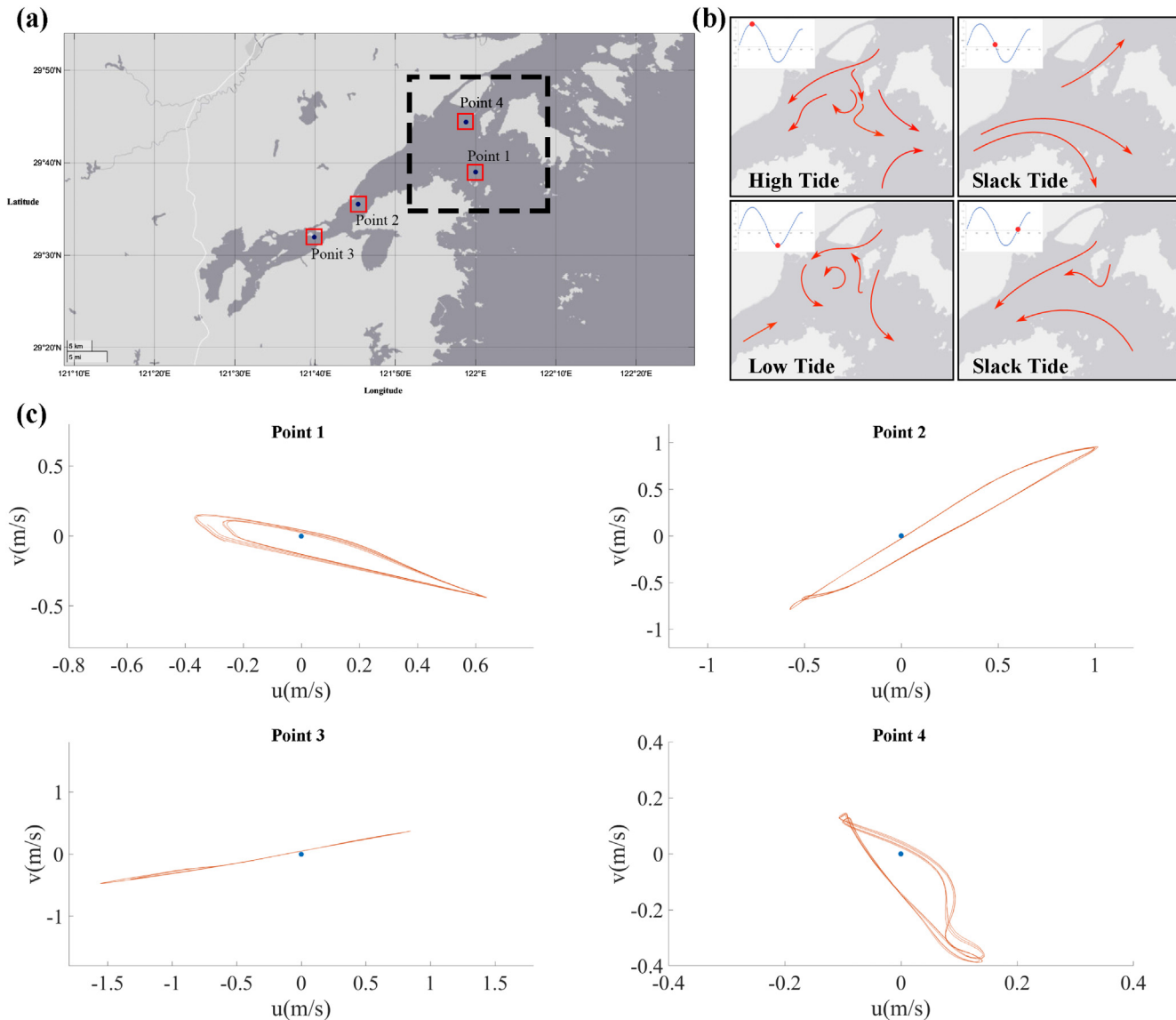


Fig. 4. Bay tidal current: (a) the geographical location of the selected flow field analysis area; (b) the schematic diagram of the flow field in the black dashed box area, the red arrow solid line represents the approximate direction of the seawater, the sub-pictures in the upper left corner of each picture indicate different tidal stages; and (c) tidal ellipse at Points 1–4, the abscissa and ordinate, respectively, indicate the velocity components in the x (longitude) and y (latitude) directions, and the solid yellow line represents the connection between the vertices of the velocity vector at different times.

The sources in the middle (S4, S5, S6, and S9) can easily affect the MP abundance of the entire bay. S7 and S8 have remarkably higher rates of retained MPs in the inner harbour area, even during high tide.

The effects of tides on the inner and outer harbours appear to be opposite. The spring tide is beneficial for the enrichment of MPs in the outer harbour area, and neap tides tend to spread MPs from the outer harbour area to both sides. This is because the velocity of the seawater changed after it passed through the narrow channel (Fig. 4c). The existence of the narrow channel leads the ebb tide to be more sensitive to the tidal range. The dots in Fig. 5b show the tidal range (abscissa) and velocity (ordinate) at different tidal stages, and the black and red lines show the correlation between the velocity and tidal range at flood and ebb tides on both sides of the narrow channel. The results showed that flow velocity was positively correlated with tidal range ($p > 0.9$). By comparing the black and red line slopes, the influence of the tidal range on the velocity of the flood tide and ebb tide can be determined. When the tidal range was small (neap tide), the velocity contrast between the inner and outer harbour areas reached a maximum, and

the flood tide velocity was greater than that of the ebb tide. The flow field was favourable for MPs to enter the inner harbour area westward. At the same time, in the process of changing from spring tide to neap tide, the tidal range decreases day by day, which is conducive to the MPs leaving the XSB. When the tidal range increased, the ebb tide speed also increased. As the tidal range increased, the ebb tide velocity in the inner port area gradually approached the flood tide velocity in the outer harbour area, which strengthened the exchange of MPs between the inner and outer harbour areas. Thus, the MPs from the inner harbour area passed through the narrow channel more easily.

The emissions at different locations and tides in the XSB significantly affect the degree of pollution. Therefore, it is necessary to formulate a reasonable scheme for MP wastewater discharge. In this study, the emissions in the inner and outer harbour areas were adjusted according to the tidal cycle. The outer harbour area is suitable as the primary discharge area; during flood and neap tide, discharge in the inner harbour area should be appropriately reduced. The Tie inlet, with a weak tidal effect, should also avoid setting up the discharge outlets.

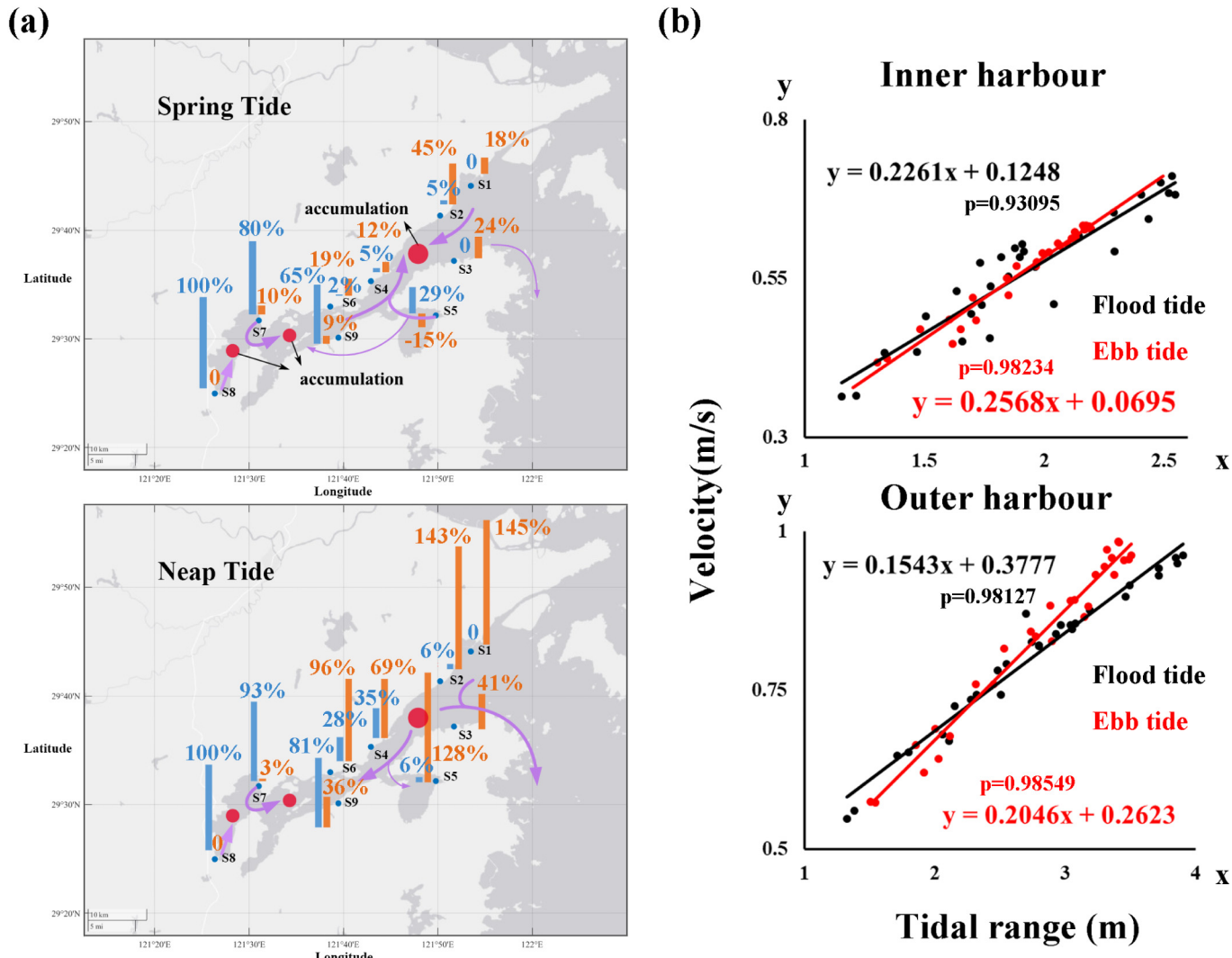


Fig. 5. (a) MPs migration during spring and neap tide (blue: the net increment of MPs in the inner harbour; and yellow: self-purification rate, percentage of MPs leaving the XSB); and (b) response of velocity on both sides of the central channel to different tidal ranges (black indicates the velocity at flood tide, and red indicates the velocity at ebb tide; 'p' is Pearson correlation coefficient).

3.2.3. Microplastics distribution in consideration of settling

The self-purification capability of the XSB achieves its weakest and strongest extremes during the spring and neap tides, respectively, and then progressively shifts to the opposite extreme when the tides change. The shift in the MP content was consistent with tidal fluctuations. There was an evident conversion from positive to negative MPs growth (SI. 5), indicating that neap tides play a significant role in purifying pollutants in the bay; however, the XSB is a high-risk region for MPs build-up. The net increase in the XSB MPs can reach >70 % in a tidal cycle, even without considering settling. Results of microplastic in sediments along the coast of the East China Sea (Zhang et al., 2020b) showed that the abundances at the bay mouth of the XSB (near S2 in our study) was higher than that outside the XSB, which showed opposite characteristics from other coastal bays (Sanmen Bay and Taizhou Bay), indicating that the MPs in the XSB may be more settled in the bay. During the simulation period, S1 showed the highest MPs migration rate, accounting for 32.06 % (SI. 6). This indicates that tidal flow is not helpful for reducing MP contamination.

MP settling is another potential factor conducive to the retention of MPs in the bay (Fig. 6). The settling velocity of MPs was estimated based on the settling formula optimised in a laboratory experiment (gravity settling under still water conditions) (Khatmullina and Isachenko, 2017). S2 (121.83°E, 29.69°N) is a site where MPs can easily depart from the bay.

After selecting the sea area near this point and considering the influence of settlement, a simple analysis was conducted (Fig. 7). First, settlement increases the abundance of MPs along the beach, and the higher the MP density, the easier it is for them to accumulate on the shore. Second, the settling effect was significant. The three settling velocities chosen (0.05, 0.1, and 0.5 mm/s) are small values estimated from the sample data. However, the MP quantities varied greatly across approximately 3.3 km (0.03° latitude). Settling weakens the tidal effects on the MPs. The shadow of the curve (Fig. 7) reflects the "fluctuations" in the abundance of MPs during rising and falling tides. The curve of the floating MPs has a larger shadow area, indicating that the horizontal diffusion distance of the floating MPs is greater during a cycle of rising and falling tides. When the settlement velocity is given, the shadow area of the curve is reduced, and the size of the shadow area is negatively correlated with the settlement velocity. The results showed that the settlement can weaken the MPs transport effect of the tide.

The self-purification rate of the XSB was barely 0.04 % when the settlement velocity exceeds 0.05 mm/s. Few samples can be calculated in this study to get such a low settling velocity of 0.05 mm/s, showing that most MPs will be deposited in the bay (except floating MPs). The accumulation of MPs is difficult. In addition to the plastic characteristics, the impacts of biofouling, upwelling, and other variables deserve further study.

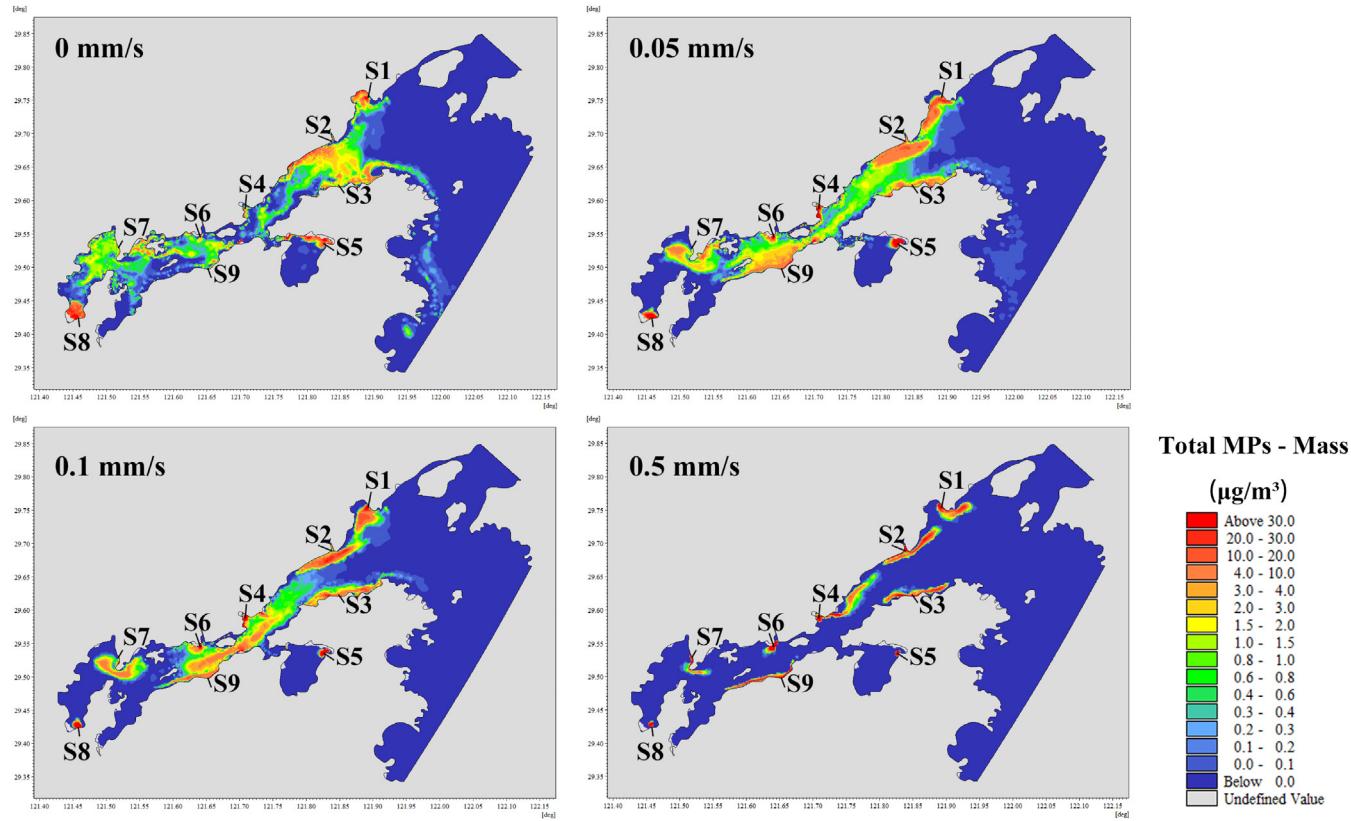


Fig. 6. MP distributions in the bay with different settling velocities. The number in the upper left corner of the image indicates the settling velocity corresponding to this result.

This study did not focus on vertical processes, and many important factors were not considered in this model. However, the settlement formula used in this paper (Khatmullina and Isachenko, 2017) was experimentally obtained in a glass water column. Further, turbulent processes are common in the ocean and affect the vertical distribution of MPs, and the MPs may oscillate in the water column because of biofouling (Kooi et al., 2017). Three-dimensional MPs transport model simulated the Sinking Characteristics of Biofouled Microplastic in the global ocean (Kooi et al., 2017; Lobelle et al., 2021), finding that particle properties combined with the global

temporal and spatial variability of physical and biological properties can result in different sinking timescales (take several to 40 days) in different regions of the ocean. The time scale of sinking depends on the density difference between the particle and the surrounding seawater, as well as downward vertical advection. As the residence time of MPs in seawater increases, consideration of only the horizontal process may be quite different from the actual situation. Exploring the influence of different vertical processes and analysing the migration of MPs in different water layers is of great significance.

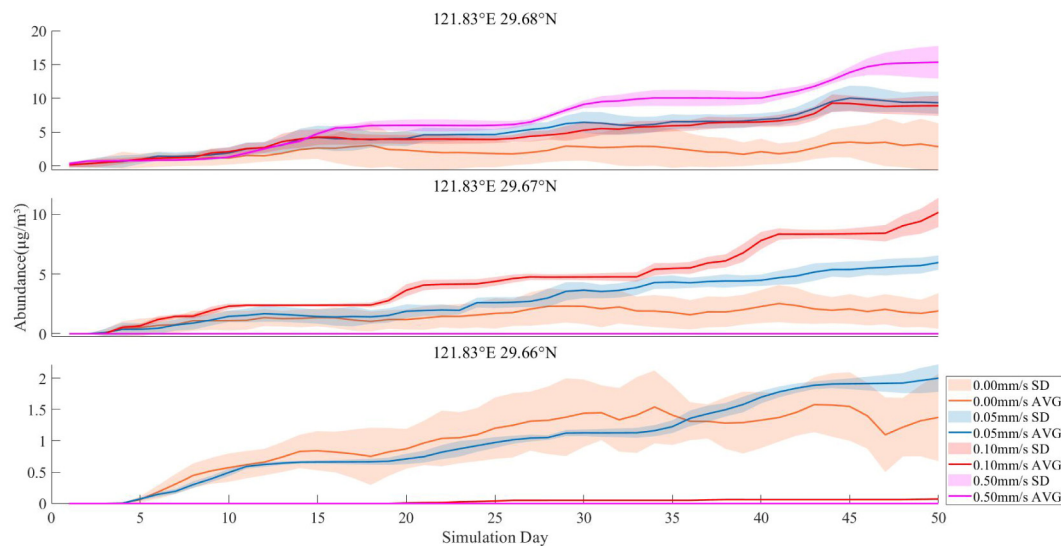


Fig. 7. MP abundance changes with the different settling velocities at three locations. The solid line represents the average abundance of MPs, and the shaded area represents the standard deviation. 29.68°N is the closest location to the north shore.

4. Conclusion

Laboratory analysis based on samples can accurately identify the chemical characteristics of MPs. In this study, we investigated the abundance, colour, shape, and polymer type of MPs based on field sampling at nine typical sites around the XSB. Numerical models with a proper set-up help study the transport of MPs. In this study, we simulated the distribution and migration of MPs under tidal forcing. The numerical simulations suggest that approximately 70 % of the MPs released at the selected sites remain in the bay after the spring and neap tides. This indicates that the XSB is a high-risk region for MPs enrichment. The numerical experiments with single-source MP release indicate that the location of the MP source determines the fate of MPs in the bay because the flow field driving MP movement is sensitive to the local topography. The narrow channel in the middle of the bay causes different MPs transport in the inner and outer harbour areas. The inner harbour tends to accumulate MPs during neap tide, and the outer harbour easily accumulates MPs during spring tide. In the case of MP settling, the accumulation of MPs in the bay is enhanced.

The narrow, semi-enclosed bay has poor water exchange and relies heavily on tides for seawater cleansing. The hydrodynamics driving MPs movement in the bay is complex. Assessing the removal and retention of MPs in the bay is of great importance. Through this study, we found that there may also be a period of MP purification in the semi-closed bay. In this study, topography changes affected seawater flow and material transport, such as narrow channels. Therefore, studying the effect of similar topography and searching for the periodic law of material transport are helpful to pollutant control in this semi-enclosed bay. Numerical models are highly effective for studying flow fields. A 2-dimension model was used in this study, although the effects of settling are discussed in part. However, the vertical velocity profiles would lead to a more complicated vertical distribution of MPs, which may result in MPs with different horizontal distributions at different depths (Wichmann et al., 2019). Meanwhile, 3-dimension models require more calibration by laboratory experiments for settling velocity and other parameters, which may be different in different open oceans or coastal seas (Lobelle et al., 2021).

CRediT authorship contribution statement

Mingchao Yin: Conceptualization, Methodology, Validation, Investigation, Data curation, Writing – original draft, Formal analysis. **Haijin Cao:** Funding acquisition, Methodology, Supervision, Project administration, Writing – review & editing. **Wenlu Zhao:** Funding acquisition, Methodology, Supervision, Writing – review & editing. **Teng Wang:** Resources, Writing – review & editing. **Wei Huang:** Methodology, Software, Resources. **Minggang Cai:** Supervision, Writing – review & editing.

Declaration of competing interest

None.

Acknowledgments

This study is supported by the National Natural Science Foundation of China (42176004, 42107268, 42107385); the Fundamental Research Funds for the Central Universities (B220202050); the Natural Science Foundation of Jiangsu Province (BK20200515); the High Performance Computing Platform, Hohai University; the Jiangsu Association for Science and Technology Young Scientific and Technological Talents Entrusted Project (JT-2022-085).

Appendix A. Supplementary data

Supplementary data to this article can be found online at <https://doi.org/10.1016/j.scitotenv.2022.157374>.

References

- Andrady, A.L., 2011. Microplastics in the marine environment. *Mar. Pollut. Bull.* 62 (8), 1596–1605.
- Aytan, U., Valente, A., Senturk, Y., Usta, R., Esenoy Sahin, F.B., Mazlum, R.E., Agirbas, E., 2016. First evaluation of neustonic microplastics in Black Sea waters. *Mar. Environ. Res.* 119, 22–30.
- Brach, L., Deixonne, P., Bernard, M., Durand, E., Desjean, M., Perez, E., van Sebille, E., ter Halle, A., 2018. Anticyclonic eddies increase accumulation of microplastic in the North Atlantic subtropical gyre. *Mar. Pollut. Bull.* 126, 191–196.
- Brennecke, D., Duarte, B., Paiva, F., Caçador, I., Canning-Clode, J., 2016. Microplastics as vector for heavy metal contamination from the marine environment. *Estuar. Coast. Shelf Sci.* 178, 189–195.
- Browne, M.A., Crump, P., Niven, S.J., Teuten, E., Tonkin, A., Galloway, T., Thompson, R., 2011. Accumulation of microplastic on shorelines worldwide: sources and sinks. *Environ. Sci. Technol.* 45 (21), 9175–9179.
- Cai, M., He, H., Liu, M., Li, S., Tang, G., Wang, W., Huang, P., Wei, G., Lin, Y., Chen, B., et al., 2018. Lost but can't be neglected: huge quantities of small microplastics hide in the South China Sea. *Sci. Total Environ.* 633, 1206–1216.
- Chen, B., Fan, Y., Huang, W., Rayhan, A.B.M.S., Chen, K., Cai, M., 2020. Observation of microplastics in mariculture water of Longjiao Bay, southeast China: influence by human activities. *Mar. Pollut. Bull.* 160, 111655.
- Chen, M., Jin, M., Tao, P., Wang, Z., Xie, W., Yu, X., Wang, K., 2018. Assessment of microplastics derived from mariculture in Xiangshan Bay.
- Chen, Z., 1992. The Bays in China (V): Bays in Shanghai And northern Zhejiang Province. China Ocean Press, Beijing (in Chinese).
- Claessens, M., Meester, S.D., Landuyt, L.V., Clerck, K.D., Janssen, C.R., 2011. Occurrence and distribution of microplastics in marine sediments along the Belgian coast. *Mar. Pollut. Bull.* 62 (10), 2199–2204.
- Cohen, J.H., Internicola, A.M., Mason, R.A., Kukulka, T., 2019. Observations and simulations of microplastic debris in a tide, wind, and Freshwater-Driven estuarine environment: the Delaware bay. *Environ. Sci. Technol.* 53 (24), 14204–14211.
- Cunningham, E.M., Ehlers, S.M., Dick, J.T.A., Sigwart, J.D., Linse, K., Dick, J.J., Kiriakoulakis, K., 2020. High abundances of microplastic pollution in Deep-Sea sediments: evidence from Antarctica and the southern ocean. *Environ. Sci. Technol.* 54 (21), 13661–13671.
- Dai, Z., Zhang, H., Zhou, Q., Tian, Y., Chen, T., Tu, C., Fu, C., Luo, Y., 2018. Occurrence of microplastics in the water column and sediment in an inland sea affected by intensive anthropogenic activities. *Environ. Pollut.* 242, 1557–1565.
- De Tender, C.A., Devriese, L.I., Haegeman, A., Maes, S., Ruttink, T., Dawyndt, P., 2015. Bacterial community profiling of plastic litter in the Belgian part of the north sea. *Environ. Sci. Technol.* 49 (16), 9629–9638.
- Ekerkes-Medrano, D., Thompson, R.C., Aldridge, D.C., 2015. Microplastics in freshwater systems: a review of the emerging threats, identification of knowledge gaps and prioritisation of research needs. *Water Res.* 75, 63–82.
- Eriksen, M., Mason, S., Wilson, S., Box, C., Zellers, A., Edwards, W., Farley, H., Amato, S., 2013a. Microplastic pollution in the surface waters of the Laurentian Great Lakes. *Mar. Pollut. Bull.* 77 (1–2), 177–182.
- Eriksen, M., Maximenko, N., Thiel, M., Cummins, A., Lattin, G., Wilson, S., Hafner, J., Zellers, A., Rifman, S., 2013b. Plastic pollution in the South Pacific subtropical gyre. *Mar. Pollut. Bull.* 68 (1–2), 71–76.
- Erofeeva, S.Y., Padman, L., Howard, S.L., 2020. Tide Model Driver (TMD) version 2.5, Toolbox for Matlab. https://www.github.com/EarthAndSpaceResearch/TMD_Matlab_Toolbox_v2.5.
- Faure, F., Saini, C., Potter, G., Galgani, F., de Alencastro, L.F., Hagmann, P., 2015. An evaluation of surface micro- and mesoplastic pollution in pelagic ecosystems of the Western Mediterranean Sea. *Environ. Sci. Pollut. Res.* 22 (16), 12190–12197.
- Gao, S., Xie, Q., Feng, Y., 1990. Fine-grained sediment transport and sorting by tidal exchange in Xiangshan Bay, Zhejiang, China. *Estuar. Coast. Shelf Sci.* 31 (4), 397–409.
- Genc, A.N., Vural, N., Balas, L., 2020. Modeling transport of microplastics in enclosed coastal waters: a case study in the Fethiye Inner Bay. *Mar. Pollut. Bull.* 150, 110747.
- Isobe, A., Iwasaki, S., Uchida, K., Tokai, T., 2019. Abundance of non-conservative microplastics in the upper ocean from 1957 to 2006. *Nat. Commun.* 10 (1).
- Jabeen, K., Su, L., Li, J., Yang, D., Tong, C., Mu, J., Shi, H., 2017. Microplastics and mesoplastics in fish from coastal and fresh waters of China. *Environ. Pollut.* 221, 141–149.
- Kaandorp, M.L.A., Dijkstra, H.A., van Sebille, E., 2020. Closing the Mediterranean marine floating plastic mass budget: inverse modeling of sources and sinks. *Environ. Sci. Technol.* 54 (19), 11980–11989.
- Kanhai, L.D.K., Gardfeldt, K., Krumpen, T., Thompson, R.C., O'Connor, I., 2020. Microplastics in sea ice and seawater beneath ice floes from the Arctic Ocean. *Sci. Rep.* 10 (1), 5004.
- Kara, L.L., Skye, M., Nikolai, A.M., Giora, P., Emily, E.P., Jan, H., Christopher, M.R., 2010. Plastic accumulation in the North Atlantic subtropical gyre. *Science* 329, 1185–1188.
- Khatmullina, L., Isachenko, I., 2017. Settling velocity of microplastic particles of regular shapes. *Mar. Pollut. Bull.* 114 (2), 871–880.
- Kooi, M., Nes, E.H.V., Scheffer, M., Koelmans, A.A., 2017. Ups and downs in the ocean: effects of biofouling on vertical transport of microplastics. *Environ. Sci. Technol.* 51 (14), 7963–7971.
- Kukulka, T., Proskurowski, G., Morét-Ferguson, S., Meyer, D.W., Law, K.L., 2012. The effect of wind mixing on the vertical distribution of buoyant plastic debris. *Geophys. Res. Lett.* 39 (7) n/a-n/a.
- Law, K.L., Morét-Ferguson, S.E., Goodwin, D.S., Zettler, E.R., Deforce, E., Kukulka, T., Proskurowski, G., 2014. Distribution of surface plastic debris in the eastern pacific ocean from an 11-year data set. *Environ. Sci. Technol.* 48 (9), 4732–4738.
- Lebreton, L., Slat, B., Ferrari, F., Sainte-Rose, B., Aitken, J., Marthouse, R., Hajjbane, S., Cunsolo, S., Schwarz, A., Levivier, A., et al., 2018. Evidence that the Great Pacific Garbage Patch is rapidly accumulating plastic. *Sci. Rep. UK* 8 (1).
- Lebreton, L.C.M., Greer, S.D., Borrero, J.C., 2012. Numerical modelling of floating debris in the world's oceans. *Mar. Pollut. Bull.* 64 (3), 653–661.

- Li, L., Guan, W., He, Z., Yao, Y., Xia, Y., 2017. Responses of water environment to tidal flat reduction in Xiangshan Bay: part II locally re-suspended sediment dynamics. *Estuar. Coast. Shelf Sci.* 198, 114–127.
- Liu, K., Zhang, F., Song, Z., Zong, C., Wei, N., Li, D., 2019. A novel method enabling the accurate quantification of microplastics in the water column of deep ocean. *Mar. Pollut. Bull.* 146, 462–465.
- Lobelle, D., Kooi, M., Koelmans, A.A., Laufkötter, C., Jongedijk, C.E., Kehl, C., van Sebille, E., 2021. Global modeled sinking characteristics of biofouled microplastic. *J. Geophys. Res. Oceans* 126 (4).
- Lusher, A.L., Tirelli, V., O'Connor, I., Officer, R., 2015. Microplastics in Arctic polar waters: the first reported values of particles in surface and sub-surface samples. *Sci. Rep. UK* 5 (1).
- Mai, L., Sun, X., Xia, L., Bao, L., Liu, L., Zeng, E.Y., 2020. Global riverine plastic outflows. *Environ. Sci. Technol.* 54 (16), 10049–10056.
- McWilliams, J.C., 2000. Chapter 14 - formulation of oceanic general circulation models. In: Randall, David A. (Ed.), *General Circulation Model Development*. Academic Press, pp. 421–456 MIKE by DHI. <http://www.mikebydhi.com>.
- Moore, C.J., 2008. Synthetic polymers in the marine environment: a rapidly increasing, long-term threat. *Environ. Res.* 108 (2), 131–139.
- National Marine Data Center, 2019. <http://mds.nmdis.org.cn/>. (Accessed 13 March 2022).
- Peeken, I., Primpke, S., Beyer, B., Gütermann, J., Katlein, C., Krumpen, T., Bergmann, M., Hehemann, L., Gerdts, G., 2018. Arctic Sea ice is an important temporal sink and means of transport for microplastic. *Nat. Commun.* 9 (1).
- Pereiro, D., Souto, C., Gago, J., 2019. Dynamics of floating marine debris in the northern Iberian waters: a model approach. *J. Sea Res.* 144, 57–66.
- Plastics Europe, 2020. Plastics – the Facts 2020. <https://plasticseurope.org/>.
- Prata, J.C., Da Costa, J.P., Lopes, I., Duarte, A.C., Rocha-Santos, T., 2020. Environmental exposure to microplastics: an overview on possible human health effects. *Sci. Total Environ.* 702, 134455.
- Reisser, J., Slat, B., Noble, K., du Plessis, K., Epp, M., Proietti, M., de Sonneville, J., Becker, T., Pattiaratchi, C., 2015. The vertical distribution of buoyant plastics at sea: an observational study in the North Atlantic Gyre. *Biogeosciences* 12 (4), 1249–1256.
- Seltenrich, N., 2015. New link in the food chain? Marine plastic pollution and seafood safety. *Environ. Health Persp.* 123 (2).
- Siegfried, M., Koelmans, A.A., Besseling, E., Kroeze, C., 2017. Export of microplastics from land to sea: A modelling approach. *Water Res.* 127, 249–257.
- Sun, X., Liang, J., Zhu, M., Zhao, Y., Zhang, B., 2018. Microplastics in seawater and zooplankton from the Yellow Sea. *Environ. Pollut.* 242, 585–595.
- Tang, G., Liu, M., Zhou, Q., He, H., Chen, K., Zhang, H., Hu, J., Huang, Q., Luo, Y., Ke, H., et al., 2018. Microplastics and polycyclic aromatic hydrocarbons (PAHs) in Xiamen coastal areas: implications for anthropogenic impacts. *Sci. Total Environ.* 634, 811–820.
- Teuten, E.L., Rowland, S.J., Galloway, T.S., Thompson, R.C., 2007. Potential for plastics to transport hydrophobic contaminants. *Environ. Sci. Technol.* 41 (22), 7759–7764.
- Tu, C., Chen, T., Zhou, Q., Liu, Y., Wei, J., Waniek, J.J., Luo, Y., 2020. Biofilm formation and its influences on the properties of microplastics as affected by exposure time and depth in the seawater. *Sci. Total Environ.* 734, 139237.
- Van Cauwenbergh, L., Vanreusel, A., Mees, J., Janssen, C.R., 2013. Microplastic pollution in deep-sea sediments. *Environ. Pollut.* 182, 495–499.
- Vianello, A., Boldrin, A., Guerriero, P., Moschino, V., Rella, R., Sturaro, A., Da Ros, L., 2013. Microplastic particles in sediments of Lagoon of Venice, Italy: first observations on occurrence, spatial patterns and identification. *Estuar. Coast. Shelf Sci.* 130, 54–61.
- Walkinshaw, C., Lindeque, P.K., Thompson, R., Tolhurst, T., Cole, M., 2020. Microplastics and seafood: lower trophic organisms at highest risk of contamination. *Ecotoxicol. Environ. Saf.* 190, 110066.
- Wang, J., Tan, Z., Peng, J., Qiu, Q., Li, M., 2016. The behaviors of microplastics in the marine environment. *Mar. Environ. Res.* 113, 7–17.
- Wang, M.H., He, Y., Sen, B., 2019. Research and management of plastic pollution in coastal environments of China. *Environ. Pollut.* 248, 898–905.
- Wang, T., Zou, X., Li, B., Yao, Y., Zang, Z., Li, Y., Yu, W., Wang, W., 2019. Preliminary study of the source apportionment and diversity of microplastics: taking floating microplastics in the South China Sea as an example. *Environ. Pollut.* 245, 965–974.
- Wang, W., Ndungu, A.W., Li, Z., Wang, J., 2017. Microplastics pollution in inland freshwaters of China: a case study in urban surface waters of Wuhan, China. *Sci. Total Environ.* 575, 1369–1374.
- Wichmann, D., Delandmeter, P., van Sebille, E., 2019. Influence of near-surface currents on the global dispersal of marine microplastic. *J. Geophys. Res. Oceans* 124 (8), 6086–6096.
- Wu, F., Pennings, S.C., Tong, C., Xu, Y., 2020b. Variation in microplastics composition at small spatial and temporal scales in a tidal flat of the Yangtze Estuary, China. *Sci. Total Environ.* 699, 134252.
- Wu, F., Wang, Y., Leung, J.Y.S., Huang, W., Zeng, J., Tang, Y., Chen, J., Shi, A., Yu, X., Xu, X., et al., 2020a. Accumulation of microplastics in typical commercial aquatic species: a case study at a productive aquaculture site in China. *Sci. Total Environ.* 708, 135432.
- Xu, P., Mao, X., Jiang, W., 2016. Mapping tidal residual circulations in the outer Xiangshan Bay using a numerical model. *J. Mar. Syst.* 154, 181–191.
- Yang, Z., Chen, J., Li, H., Jin, H., Gao, S., Ji, Z., Zhu, Y., Ran, L., Zhang, J., Liao, Y., et al., 2018. Sources of nitrate in Xiangshan Bay (China), as identified using nitrogen and oxygen isotopes. *Estuar. Coast. Shelf Sci.* 207, 109–118.
- Yu, X., Huang, W., Wang, Y., Wang, Y., Cao, L., Yang, Z., Dou, S., 2022. Microplastic pollution in the environment and organisms of Xiangshan Bay, East China Sea: an area of intensive mariculture. *Water Res.* 212, 118117.
- Zhang, C., Zhou, H., Cui, Y., Wang, C., Li, Y., Zhang, D., 2019. Microplastics in offshore sediment in the Yellow Sea and East China sea, China. *Environ. Pollut.* 244, 827–833.
- Zhang, F., Yao, C., Xu, J., Zhu, L., Peng, G., Li, D., 2020b. Composition, spatial distribution and sources of plastic litter on the East China Sea floor. *Sci. Total Environ.* 742, 140525.
- Zhang, W., Zhang, S., Wang, J., Wang, Y., Mu, J., Wang, P., Lin, X., Ma, D., 2017. Microplastic pollution in the surface waters of the Bohai Sea, China. *Environ. Pollut.* 231, 541–548.
- Zhang, Z., Wu, H., Peng, G., Xu, P., Li, D., 2020a. Coastal ocean dynamics reduce the export of microplastics to the open ocean. *Sci. Total Environ.* 713, 136634.
- Zhao, S., Zhu, L., Wang, T., Li, D., 2014. Suspended microplastics in the surface water of the Yangtze Estuary System, China: first observations on occurrence, distribution. *Mar. Pollut. Bull.* 86 (1–2), 562–568.
- Zhao, W., Huang, W., Yin, M., Huang, P., Ding, Y., Ni, X., Xia, H., Liu, H., Wang, G., Zheng, H., et al., 2020. Tributary inflows enhance the microplastic load in the estuary: a case from the Qiantang River. *Mar. Pollut. Bull.* 156, 111152.
- Zheng, Y., Li, J., Cao, W., Liu, X., Jiang, F., Ding, J., Yin, X., Sun, C., 2019. Distribution characteristics of microplastics in the seawater and sediment: a case study in Jiaozhou Bay, China. *Sci. Total Environ.* 674, 27–35.
- Zhu, J., Zhang, Q., Li, Y., Tan, S., Kang, Z., Yu, X., Lan, W., Cai, L., Wang, J., Shi, H., 2019. Microplastic pollution in the Maowei Sea, a typical mariculture bay of China. *Sci. Total Environ.* 658, 62–68.